Wavelet transform modulus maxima and holder exponents combined with transient detection for the differentiation of pitting corrosion using electrochemical noise

Homborg, A. M.; Oonincx, P.J.; Mol, J. M.C.

DOI
10.5006/2788

Publication date
2018

Document Version
Accepted author manuscript

Published in
Corrosion

Wavelet transform modulus maxima and Holder exponents combined with transient detection for the differentiation of pitting corrosion using electrochemical noise

A.M. Homborg,[*,***] *P.J. Oonincx,*[*] *and J.M.C. Mol,*[**]

ARTICLE INFO

Article history:

Received: February 15, 2018
Revised: April 11, 2018

Keywords:

A. Electrochemical noise
B. Pitting corrosion
C. Transient analysis
D. Wavelet transform modulus maxima
E. Holder exponent

[*] Netherlands Defence Academy, AM.Homborg@mindef.nl; PJ.Oonincx@mindef.nl, P.O. Box 10000, 1780CA Den Helder, The Netherlands

[**] Delft University of Technology, Department of Materials Science and Engineering, J.M.C.Mol@tudelft.nl, Mekelweg 2, 2628CD Delft, The Netherlands

[***] Corresponding author: +31 223 657558, AM.Homborg@mindef.nl

ABSTRACT

A potentially powerful tool to detect and classify corrosion mechanisms is the analysis of electrochemical noise (EN). Data analysis in the time-frequency domain using e.g. continuous wavelet transform (CWT) allows the extraction of localized frequency information, providing information on the type of corrosion, i.e. uniform or localized corrosion, from the EN signal. The CWT provides the opportunity to analyse changes in frequency behavior of electrochemical noise signals over time. In the presence of transients generated by pitting corrosion that occur only during short instants of time, this is an important property. This paper introduces the combination of automated transient detection with wavelet transform modulus maxima (WTMM) and the Holder exponent. WTMM enhances the determination of transient frequencies by indicating the ridges of a CWT spectrum. The Holder exponent, a measure of singularity of an EN signal, provides a single parameter discrimination tool based on WTMM and serves to differentiate between general corrosion and two types of pitting corrosion of stainless steel AISI304 exposed to aqueous HCl solutions of different concentrations and as such at different pH values.

INTRODUCTION

Electrochemical noise (EN), or spontaneous fluctuations in current and potential, is generated by charge transfer reactions that are caused by electrochemical metal dissolution processes. The measurement of EN is already performed by corrosion researchers for decades [1]. The first reports from the study of EN date from the 1960s, when Hagyard and Williams [2] and Iverson [3] investigated electrochemical potential signatures that were related to corrosion. The occurrence of localized corrosion and its relation with specific fluctuations in the electrochemical potential noise was then published by Hladky and Dawson [4, 5]. These specific localized features in the EN signal are defined as transients. Although this work discusses the analysis of transients under open-circuit conditions, the investigation of EN transients under cathodic or anodic polarization is also reported [6-8]. Each transient can be associated with specific frequency information in the EN signal, reflecting the nature of the corrosion process. One of the most challenging possibilities of EN is the identification of localized corrosion processes based on the characteristics of these transients [9-14].

Although the measurement technique has remained largely unchanged, many different data analysis procedures have been proposed to extract the desired information [15]. Classical spectral analysis of EN can be done using the well-known Fourier transform, which can be regarded as the most direct way to estimate a power spectrum [1]. However, corrosion processes are typically nonlinear and non-stationary. Non-stationarity becomes visible in the presence of a DC drift in the EN signal, hence the mean value changes over time. Strictly spoken, some of the commonly applied data analysis methods are not suitable for EN. The calculation of (spectral) noise resistance or any parameter derived from the power spectral density assumes a stationary process and thus requires the removal of the DC drift or windowing beforehand [1, 16-19].

A different way to analyse EN signals is the application of time-frequency techniques [20, 21]. The analysis of time-frequency information of EN offers some important advantages over the widely used Fourier transform [22]. Most important is the absence of the criterion that the EN signal should be stationary. In this paper we introduce a method to obtain physical information and quantify it from noise data. The method is based on a rigorous analysis of the irregularities in the noise data, that can be interpreted as discontinuities of the underlying mathematical function. In the analysis of EN, irregularities can be regarded as the transients that occur due to the underlying physico-chemical process. Metastable pitting of stainless steel, for example, generates clearly distinguishable irregularities, or transients, in the EN signal [20]. Traditionally Fourier analysis is used to analyze irregular behavior of signals. However, the disadvantage when using Fourier analysis is that the information on local behavior in the signal is lost because the resulting frequency spectrum captures the entire signal. Any small events visible in the time domain are therefore likely to be lost in the frequency domain. For non-stationary signals traditional frequency analysis becomes inappropriate because of this property.

In many other papers the Discrete Wavelet Transform (DWT) has been used for analyzing EN signals [9, 18, 21, 23-28], firstly introduced for the analysis of EN by Aballe et al. [21]. The DWT describes the original EN signal using a linear combination of oscillations with a limited time span, called wavelets. In the first stage, a so-called 'mother wavelet' is moved along the EN signal and correlated with it. This results in a set of wavelet coefficients for this specific wavelet size (or scale). Subsequently, the mother wavelet is scaled up by a certain factor, in order to make it longer, and the correlation process is repeated. Due to the scaling process, after each iteration, lower frequencies are described. In other words, DWT analyses the EN signal using a pre-defined number of timescales by scaling and translation of wavelets [9, 18, 21, 23-28]. The energy present in those timescales could in turn be associated with the dominance of activation- or diffusion controlled processes, or processes under mixed control [7, 9, 16, 18, 21, 23-30]. Larger timescales are related with relatively slow processes, whereas smaller timescales are related to faster processes [18, 24-26, 28]. The relation between spectral and wavelet techniques for the analysis of EN has been described earlier by Cottis [22]. The DWT combines several interesting properties of the Fourier transform. It offers a fast algorithm to decompose signals in uncorrelated components that represent irregularities from the data at several scales / frequencies. This property has already proven itself to be a very useful analyzing tool for several physical problems including in the field of corrosion. The DWT is a fast way to analyze irregular behavior because it does not include all frequencies of the irregularities that can be observed. It is a multiscale analysis at dyadic scales (i.e. scales that increase each time by a ratio of two) yielding a wide spread of the irregular features in the time-scale domain. This spreading results in the problem of properly identifying the irregularities in the time-scale domain. A solution to this problem would be to consider irregularities at all scales / frequencies, i.e., without dyadic sampling. This can be achieved by using the Continuous Wavelet Transform (CWT) [31]. A different data analysis method in the time-frequency domain offering the possibility to visualize the change in frequency characteristics over time is the Hilbert-Huang transform (HHT) [20, 32]. As an example of the application of HHT to the analysis of EN signals, it is used to identify corrosion inhibition [33] or microbiologically influenced corrosion [34]. One of the most important challenges that can be overcome by using time-frequency data analysis methods is the ability of these techniques to analyse individual transients generated by localized corrosion processes [35]. This ability however introduces a new issue, since the typical spread of low frequency information over time in a CWT spectrum can impede the association of this localized frequency information with specific transients. The resolution in time can be improved, but this then goes at the expense of losing resolution in frequency [22].

The wavelet transform modulus maxima (WTMM) procedure describes the evolution of wavelet maxima across scales and can be used to identify singularities, or transients, present in a signal [36-40]. WTMM has found some interesting applications in various different fields of technology, including e.g. vibration analysis [41], 3D depth estimation [42], detection of specific features in ECGs [43] or structural health monitoring [44, 45]. Besides the employment of real-valued wavelets, also WTMM of complex-valued wavelets can be used for the estimation of instantaneous frequencies and detection of transients in a signal [46].

Once the WTMM are described, it is useful to quantify their decay across the scales. A transient, that is in fact a large change in the signal, will have large coefficients in the CWT spectrum at the different scales, and therefore little decay across the spectrum compared to other parts of the signal. This decay is described by the Holder, or Lipschitz exponent [40]. The local Holder exponent indicates the local singularities present in a signal. The global Holder exponent provides an overall value of singularity of the entire signal. At locations with high local Holder exponents, the signal is expected to be smoother than compared to locations with low local Holder exponents. A local Holder exponent of 0 or a negative value indicates a discontinuity in the signal. On the other hand, a signal that is locally differentiable (i.e. 'smooth') produces a local Holder exponent of 1 or higher. Holder exponent

values between 0 and 1 indicate that the signal is continuous, but not differentiable. Within this range, the Holder exponent ranges from indications of strong singularity (close to 0) to almost differentiable (close to 1). Singularity detection using the Holder exponent can e.g. be used in applications such as structural health monitoring [47] and image processing for the removal of noise [48]. By comparing this local singularity between EN signals from different pitting corrosion processes, the present work investigates whether it is possible to use this parameter as a differentiation criterion for corrosion.
To facilitate the analysis of EN transient frequency information in CWT spectra, the present work introduces the WTMM method. In addition to the WTMM, the Holder exponent is used here to analyse the strength of the singularities. In order to indicate the effectiveness of the use of WTMM and Holder exponents for differentiation between corrosion mechanisms, three data sets are used. Each data set consists of EN measurements performed on AISI304 stainless steel, exposed to aerated HCl solutions ranging from pH 1.0 to pH 3.0. The resulting corrosion processes of the AISI304 therefore differ for each data set, as the authors described in earlier work [20]. These material-electrolyte combinations are selected, because the results are well-defined corrosion characteristics, which were investigated by the authors earlier using the HHT and reported elsewhere [20, 35]. It is therefore the primary objective of the current work to introduce the novel data-analysis procedure with the application of modulus maxima and the Holder exponent combined with transient analysis, and to investigate its rubustness using these well-known corrosion processes.

Experimental

Materials and experimental set-up

The experimental setup is identical to the one described in [35]. The experiments comprise of two identical AISI304 working electrodes and one reference electrode, type Radiometer analytical Red Rod REF201 (Ag/AgCl/sat. KCl: 0.207 V vs. SHE). The working electrode area was 0.05 cm^2. The working electrodes were exposed to the electrolyte after being stored under ambient conditions at 20°C for 24 h and microscopically inspected for irregularities. Three different aqueous HCl solutions served as electrolytes, with concentrations of 0.1, 0.01 and 0.001M. The pH values were 1.0, 1.9 and 3.0, respectively. A Faradic cage served to prevent any electromagnetic interference during the measurements. The working electrode surfaces were microscopically inspected afterwards using an optical microscope with a maximum magnification of 1000x.
A Compactstat from Ivium Technologies was used to record electrochemical current- (ECN) and potential noise (EPN) signals, working as zero resistance ammeter and potentiometer. The Compactstat was controlled by a Windows-based PC running dedicated software. The sampling frequency for the measurements described in this work was set at 5 Hz, with the application of a low-pass filter of 10 Hz. The only significant additional noise source between the Nyquist frequency (2.5 Hz in this case) and the frequency of the low-pass filter was considered to be instrumental noise generated by this instrument, and was therefore closely investigated. For this procedure, a method introduced by Ritter et al. [49] was applied: EN signals were recorded for a selection of different pure Ohmic resistances and the level and overlap of their power spectral densities at different sampling rates was verified. The 'remove DC initial' option of the device was applied, i.e. the first data point of the EPN signal was set to zero using a pre-defined offset prior to data acquisition. This allowed the measurement device to narrow the potential range and to enhance the resolution of the recorded signal. Matlab from MathWorks was used as data processing software.
The CWT for the time-frequency spectra used an analytic Morlet wavelet. This wavelet applies the discrete Fourier transform algorithm [50]. An important procedure when calculating the CWT is to make sure that the wavelet overlaps the beginning and end of the EN signal by half its duration when it calculates the first and last points of the spectrum. This is also known as padding, by which the EN signal is actually extended at the beginning and end. The padding methods that can be applied in Matlab are described in detail in [51]. Without choosing the correct padding procedure, artifacts may arise at the beginning and end of the spectrum. In earlier work [31], symmetric padding had been selected as most suitable for the analysis of EN signals. Finally, the calculation of the CWT used 32 voices per octave, i.e. for each factor of two frequency range, 32 frequencies with logarithmic spacing were calculated. For the WTMM, the Matlab default second derivative of a Gaussian wavelet was applied.

Wavelet transform modulus maxima and Holder exponent

For the determination of transient locations in EN signals one can use various type of methods that from a mathematical point of view deal with detecting discontinuous and non-differentiable data. In this paper we do not only want to detect singularities (i.e. transients) in data, but also try to classify them in order to use the mathematical approach as a method to differentiate between corrosion mechanisms.

A well-known approach in mathematics to describe the local regularity of a function x(t) in a small neighbourhood of time t_0 is to use its Taylor expansion into a polynomial $p_N(t-t_0)$ of degree N and to study the approximation error. From this we get the definition of the Holder exponent $\alpha \geq 0$, i.e., a function x(t) has Holder exponent $\alpha \geq 0$ at t_0 if there exists a constant $C>0$ and a polynomial p_N of degree N such that [52]

$$|x(t) - p_N(t - t_0)| \leq C\,|t - t_0|^{\alpha} \quad (1)$$

To understand this equation one can substitute different values for α at the right hand side. For α=0 we observe that the approximation error is bounded independent of the value of t, while for α>0 the error will tend to zero as t→ t_0. Clearly, the Holder exponent α is a measure of local regularity of a signal x(t) in a neighbourhood of time sample t_0.

In [22] the CWT has already been introduced for the analysis of transients in EN signals. An important property of the CWT can be related to the determination of the Holder exponent in irregular signals. For this we recall the definition of the CWT for a signal x(t) [53]

$$W_{\psi}[x](s,b) = \int x(t)\psi\left(\frac{t-b}{s}\right)dt \qquad (2)$$

The analysing wavelet ψ is said to have N vanishing moments if $W_{\psi}[p_k]=0$ for all polynomials p_k of degree k≤N. In practice this means that the wavelet transform is 'blind' for the linear trend in the signal in case N=1 and for curvy trends in case of more vanishing moments. Because of this property the CWT is able to detect irregularities superposed on trend like behavior of a signal.

In [54] Jaffard deduced the following result from elementary mathematical theorems:

$$\left|W_{\psi}[x](s,t_0)\right| \leq As^{\alpha+1/2} \qquad (3)$$

with constant A≥0 and for wavelets with a substantial amount of vanishing moments. Without going too much into the detail of this theorem, proving the result is based on applying the CWT in (1) using the fact that $W_{\psi}[p_N]=0$. From the latter equation it is obvious that applying the CWT yields a mathematical expression between each individual time sample t_0 and the Holder exponent α as a parameter of local regularity. Taking the $\log_2$ of the left and right hand side of the inequality yields

$$\log_2\left|W_{\psi}[x](s,t_0)\right| \leq \log_2 A + \left(\alpha + \frac{1}{2}\right)\log_2 s \qquad (4)$$

The choice for using $\log_2$ instead of ln or other logarithms is given by the fact that scales s in the CWT are always computed in a dyadic manner. The Holder exponent α can now be computed (up to a constant ½) by considering the decay slope of $\log_2 |W_{\psi}[x](s,t_0)|$ as a function of $\log_2 s$.

For computing the exponent the Wavelet Transform Modulus Maxima (WTMM) is used as a procedure to analyse wavelet maxima across scales. The ridges and their slopes in particular are used to compute the Holder exponent related to the singularity at time sample t_0

The principle of selecting WTMM for the determination of the Holder exponent is based on the procedure of transient analysis, as presented by the authors in earlier work [35]. This method allows the determination of transient locations in the EN signal. The purpose of transient analysis is to allow detailed investigation of the areas in time-frequency spectra that are associated with the occurrence of transients. By selecting only those areas of interest, either the individual transients can be investigated by their instantaneous frequency composition, or the instantaneous frequencies of multiple transients can be averaged. The latter is intended for the investigation of overall corrosion characteristics in the case of localized corrosion. In the present work, the procedure of transient selection is based on the EPN signal. First the peak of each transient is detected automatically, using the difference between the EPN signal and a moving average of the EPN signal. From this difference, the extrema are indicated as the transient peaks. As a second step, from each peak to the left the transient start is associated with the location where the absolute value of the amplitude of the EN signal starts to increase. Finally, the transient end is determined as the location where the amplitude reaches back to the original value again. After this operation has been completed for all transients in the EN signal, the corresponding ridges in the CWT spectrum, indicated by the WTMM, are selected. By this way, for each WTMM of interest, the corresponding Holder exponent is analysed. All other Holder exponents, describing the singularity of the EN signal in between the transients, are neglected. Holder exponents that are associated with transients are averaged for each EPN signal. In the case of the EPN signals from AISI304 exposed to HCl at pH 1.0, the general corrosion attack results in the absence of transients. Here, the global Holder exponent is used as an indication of (non)singularity of the entire EPN signal. In all other cases, the local Holder exponent is used.

Results and discussion

Analysis of modulus maxima and Holder exponents

Figure 1 shows examples of micrographs of the AISI304 after exposure to the three different concentrations of HCl for a duration of 1000s. This indicates the difference in pitting severity between the three different electrolytes.

Figure 1

The micrograph of Figure 1a shows the lowest number of pits after the exposure to HCl at pH 3.0, together with a relatively smooth working electrode surface. Careful examination of the working electrode areas using optical microscopy revealed no corrosion attack in between the locations of the pits. Figure 1b indicates that after the exposure to HCl at pH 1.9, a larger number of pits arises, again on an otherwise smooth working electrode surface, with the pre-processing marks still visible. Finally, at pH 1.0, Figure 1c shows that the working electrodes undergo a general corrosion attack, which also concentrates at certain shallow spots. Those spots appear notably darker in the micrograph. Contrary to the working electrodes shown in Figure 1a and 1b, instead of a smooth appearance of the areas in between those spots, the working electrode surface is largely corroded.

Figure 2 shows an EPN signal of a measurement on AISI304, exposed to an HCl solution at pH 3.0 (a), 1.9 (b) and 1.0 (c) for a duration of 1000s. In case of the presence of transients, the transient locations are indicated in blue.

Figure 2

Figure 2a and 2b show the presence of transients. These transients could be associated with the existence of pits at the working electrode surfaces [35]. For pH 1.0, the EN signals generated by this type of corrosion however do not contain any transients and they exhibit a relatively smooth character [35]. This is shown in the example Figure 2c. For this reason, the EPN signals for AISI304 exposed to HCl at pH 3.0 and 1.9 from Figure 2a and 2b will serve as examples to explain the analysis procedure in this section. The final analysis of the experimental results includes the Holder exponents of the corrosion characteristics at all three pH values.
The transient locations defined in Figure 2a and 2b are used for the determination of the Holder exponents of interest. These transients are generated by the pitting processes at the working electrode surfaces. The first stage of a potential transient indicates pit initiation [55]. Subsequently, pits grow in a metastable stage for a period from several seconds to several tens of seconds, by undermining the passive film that is present at the surface to protect the stainless steel [56, 57]. This stage is under diffusion control and the Ohmic resistance of the pit cover plays a determining role here [56, 58]. This Ohmic resistance is generated by the current inhibition, or the inhibition of metal ion flow out of the pit and electrolyte flow in and out of the pit, through pores in the pit cover [56, 59]. The drop in the potential is the result of this increased Ohmic resistance, combined with the fact that the current density is constant over the lifetime of the pit [55, 56, 60]. Repassivation occurs when the pit cover is penetrated [56]. Repassivation is a fast process, after which the passive film slowly regenerates [56]. The second part of the potential transient, which is characterized by a decrease of the absolute amplitude, is associated with the discharge of the interface capacity, which occurs after repassivation [55].
The EN signal displayed in Figure 2b shows a larger number of blue transient indicators, and hence a larger number of pitting events, than compared to the EN signal from Figure 2a. The corrosive environment at pH 1.9 is more aggressive for AISI304, with a less stable oxide layer and more undermining per unit surface area as a result. The pitting process generating the EN signal in Figure 2b is therefore more severe and the EN signal contains a larger number of transients. Because of the large number of transients in the EN signal of Figure 2b, some are close together and it is difficult to visually determine those transient locations. For this purpose, Figure 3 shows an enlargement of two sections of each 60s duration of the EN signal of Figure 2b: 120-180s (left hand side) and 800-860s (right hand side).

Figure 3

Figure 3 indicates that, although some transient locations are close together, all detected transient locations are at a local minimum of the EPN signal, as expected.
For the analysis procedure proposed in this work, first the CWT spectra are produced, as shown in Figure 4. In a CWT spectrum, the energy distribution of the EN signal over time and scale is visualized. For convenience, the scales are converted into frequencies, as indicated at the x-axis.

Figure 4

The notable difference between the frequency range of the maxima in these spectra was already discussed by the authors in earlier work, based on Hilbert spectra [20]. The CWT spectrum displayed in Figure 4a shows maxima between 10^{-1} and 10^{-2} Hz. On the contrary, the CWT spectrum in Figure 4b has maxima at the low frequency end of the CWT spectrum (around $4 \bullet 10^{-3}$ Hz in this case). The reason for this is greater stability of the oxide film in the case of Figure 4a, with a reduced influence of oxygen diffusion on the corrosion process as a result [25, 26]. Figure 2a showed a smaller number of transients as compared to the EN signal of Figure 2b. This,

together with a larger relative contribution of instantaneous frequencies in the range between 10^{-1} and 10^{-2} Hz, is indicative of a more stable oxide film in the case of Figure 4a [61].

Another apparent characteristic of the CWT spectrum of Figure 4b is the spread of the low frequency information over time. As mentioned in the introduction, this phenomenon is difficult to avoid without sacrificing resolution in frequency [22]. This spread can also impede a correct interpretation of the localized frequency information that can be associated with transients. The combination of the calculation of WTMM with the automated transient analysis procedure is intended to overcome this problem and to enable a full localized frequency investigation for each transient.

After the determination of the CWT spectrum, the WTMM are defined. Figure 5 shows the WTMM as an overlay with black markers on top of the CWT spectra from Figure 4, together with their two-dimensional representations.

Figure 5

The CWT spectrum of Figure 5a shows that the WTMM corresponding to the ridges that are generated by the EN transients exist over a larger frequency range than compared to WTMM that are associated with locations in between the transients. A three-dimensional representation has the advantage to rotate the CWT spectrum into different perspectives, which can emphasize local frequency amplitudes that are otherwise difficult to distinguish using only the colour markings. This especially accounts for local frequencies that are generated by small transients. However, depending on the perspective of a three-dimensional plot, the exact location of WTMM can be difficult to determine. Hence, Figure 5b and 5d also provides two-dimensional plots of the CWT spectra.
The visual inspection of WTMM as shown in Figure 5b and 5d can be useful to determine the frequency range of individual transients, such as the single large transient around t=550s, visible in Figure 2a. This transient is associated with the largest amplitudes in the CWT spectrum in Figure 4a, and the WTMM in Figure 5b indicate that the frequency range of this particular transient extends down to approximately $4 \bullet 10^{-3}$ Hz.

After the determination of WTMM, in order to be able to differentiate between EN signals from different corrosion processes, it is useful to quantify this information in a single parameter. Therefore, the Holder exponent of each transient is calculated. This results in a collection of Holder exponents, where each one is representative for a single pitting process that occurred at the working electrodes. The mean value of these Holder exponents thus expresses an overall indication of the type of pitting based on selected areas of the time-frequency spectrum, despite the instantaneous nature of a pitting process. Table 1 presents these Holder exponents for the two EN signals under investigation.

Table 1

There is a clear difference between the Holder exponents of the two EPN signals. This difference originates from the typical mechanistic distinction between the two associated pitting processes. With the decrease in pH from 3.0 to 1.9, the duration of the transients becomes larger. The largest amplitudes in the CWT spectra shift to a lower frequency range. This was visible in the maxima of the CWT spectrum in Figure 4b as compared to those in Figure 4a. It can be argued that the transients in the EPN signal of Figure 2b contain less sharp transitions than compared to those of the EPN signal of Figure 2a. This originates from the fact that the pits at pH 1.9 arise on a surface with a less stable oxide film (EPN signal in Figure 2b) than compared to those at pH 3.0 (Figure 2a). As discussed before, as the stability of the oxide film increases, the influence of (slow) oxygen diffusion on the corrosion process reduces [25, 26]. In mathematical terms, the transients in Figure 2b are less singular, and therefore increasingly differentiable, than those in Figure 2a.

Data set results
In the previous section, the two different pitting processes could be clearly distinguished based on the Holder exponent as a single parameter analysis, with a proper relation with the underlying physico-chemical mechanism. In this section, the robustness of the proposed analysis procedure of transient identification, CWT, WTMM and finally the Holder exponent will be investigated based on three data sets, AISI304 exposed to an aqueous HCl solution at pH 1.0, 1.9 and 3.0, also incorporating the two example EPN signals as used in the previous section. Figure 6 shows the mean local (pH 3.0 and 1.9) or global (pH 1.0) Holder exponents of all EPN signals, indicated by the square markers.

Figure 6

Figure 6 indicates that the three different pH values result in EN signals with notably different singularities. This difference is clarified further by the horizontal lines that represent the mean value of all Holder exponents for each of the three data sets. The three different average values of the Holder exponents is in good accordance

with earlier experimental observations for the associated corrosion processes [35]. As was explained in the introduction, at locations with high local Holder exponents, the EN signal is expected to be smoother than compared to locations with low local Holder exponents. Discontinuities in the EN signal generate a local Holder exponent of 0 or a negative value, whereas a local Holder exponent of 1 or higher can be associated with an EN signal that is locally differentiable, or 'smooth'. If the EN signal is continuous, but not differentiable, the Holder exponent ranges between 0 (strong singularity) and 1 (almost differentiable). At pH 1.0, the average Holder exponent lies above 1, indicating a locally differentiable signal. In the absence of transients at this pH value, indeed the EN signals have a 'smooth' character [35]. At pH 1.9, the average Holder exponent is approximately 0.62 and at pH 3.0 this value decreases to approximately 0.17. As was discussed for the data shown in Table 1, with the decrease in pH from 3 to 1.9, the duration of the transients becomes larger. This was made visible in Figure 4, with a shift of the largest amplitudes in the CWT spectra to a lower frequency range. The transients in the EN signals at pH 1.9 therefore contain less sharp transitions than compared to those at pH 3.0. Figure 2 showed an example of this difference. The transients at pH 3.0 are thus more singular and less differentiable than those at pH 1.9.

For further quantification of the differentiation ability of this procedure, Figure 7 shows Gaussian curves for each of the three data sets. Here, the probability density of a Holder exponent for the three experimental conditions under investigation (pH 1.0, 1.9 or 3.0) is provided. In addition, the original Holder exponents from Figure 6, used for the calculation of each Gaussian curve, are shown at the x-axis.

Figure 7

The Gaussian curves shown in Figure 7 indicate that, although there is overlap in probability density for these three experimental conditions, this occurs only at the outer edges of the probability density curves. This implies that the Holder exponent has good discrimination ability for the general and two types of pitting corrosion of AISI304 in aqueous HCl at pH 1.0, 1.9 and 3.0.

Conclusions

Based on the known differences between the general and localized corrosion processes of AISI304 exposed to an HCl electrolyte at pH 1.0, 1.9 and 3.0, a novel data analysis procedure of EN signals has been proposed. The combination of transient selection and analysis, wavelet transform modulus maxima (WTMM) and calculation of the Holder exponent has shown to be a robust tool to differentiate between general corrosion attack and different forms of pitting corrosion of AISI304 exposed to an aqueous HCl solution.
WTMM effectively indicate the frequency range of each transient visible in the continuous wavelet transform (CWT) spectrum. Furthermore, WTMM can be a useful tool for correct interpretation of time-frequency information in a CWT spectrum in the low frequency range, where the energy of an electrochemical noise signal is less localized in time.

Acknowledgements

Endures BV in Den Helder, The Netherlands, is gratefully acknowledged for accommodating the research work.

References

[1] R.A. Cottis, Interpretation of electrochemical noise data, Corrosion, 57 (2001) 265-285.
[2] T. Hagyard, J.R. Williams, Potential of aluminium in aqueous chloride solutions, Part 1, Trans. Faraday Soc., 57 (1961) 2288-2294.
[3] W.P. Iverson, Transient voltage changes produced in corroding metals and alloys, J. Electrochem. Soc., 115 (1968) 617-618.
[4] K. Hladky, J.L. Dawson, The measurement of localized corrosion using electrochemical noise, Corros. Sci., 21 (1981) 317-322.
[5] K. Hladky, J.L. Dawson, The measurement of corrosion using electrochemical 1/f noise, Corros. Sci., 22 (1982) 231-237.
[6] H.S. Klapper, J. Goellner, A. Heyn, The influence of the cathodic process on the interpretation of electrochemical noise signals arising from pitting corrosion of stainless steels, Corros. Sci., 52 (2010) 1362-1372.
[7] J.J. Kim, Wavelet analysis of potentiostatic electrochemical noise, Mater. Lett., 61 (2007) 4000-4002.
[8] C. Aldrich, B.C. Qi, P.J. Botha, Analysis of electrochemical noise data with phase space methods, Miner. Eng., 19 (2006) 1402-1409.
[9] A. Aballe, M. Bethencourt, F.J. Botana, M. Marcos, J.M. Sánchez-Amaya, Use of wavelets to study electrochemical noise transients, Electrochim. Acta, 46 (2001) 2353-2361.
[10] Q. Hu, G. Zhang, Y. Qiu, X. Guo, The crevice corrosion behaviour of stainless steel in sodium chloride solution, Corros. Sci., 53 (2011) 4065-4072.

[11] M. Breimesser, S. Ritter, H. Seifert, T. Suter, S. Virtanen, Application of electrochemical noise to monitor stress corrosion cracking of stainless steel in tetrathionate solution under constant load, Corros. Sci., 63 (2012) 129-139.
[12] C. Gabrielli, M. Keddam, Review of applications of impedance and noise analysis to uniform and localized corrosion, Corrosion, 48 (1992) 794-811.
[13] S.V. Muniandy, W.X. Chew, C.S. Kan, Multifractal modelling of electrochemical noise in corrosion of carbon steel, Corros. Sci., 53 (2011) 188-200.
[14] R.A. Cottis, Simulation of electrochemical noise due to metastable pitting, J. Corros. Sci. Eng., 3 (2000) 1-9.
[15] A.M. Homborg, T. Tinga, E.P.M. van Westing, X. Zhang, G.M. Ferrari, J.H.W. de Wit, J.M.C. Mol, A Critical Appraisal of the Interpretation of Electrochemical Noise for Corrosion Studies, Corrosion, 70 (2014) 971-987.
[16] B.D. Malamud, D.L. Turcotte, Self-affine time series: measures of weak and strong persistence, Journal of Statistical Planning and Inference, 80 (1999) 173-196.
[17] U. Bertocci, F. Huet, R.P. Nogueira, P. Rousseau, Drift removal procedures in the analysis of electrochemical noise, Corrosion, 58 (2002) 337-347.
[18] Z. Dong, X. Guo, J. Zheng, L. Xu Calculation of noise resistance by use of the discrete wavelets transform, Electrochem. Commun., 3 (2001) 561-565.
[19] F. Mansfeld, Z. Sun, C.H. Hsu, A. Nagiub, Concerning trend removal in electrochemical noise measurements, Corros. Sci., 43 (2001) 341-352.
[20] A.M. Homborg, E.P.M. van Westing, T. Tinga, X. Zhang, P.J. Oonincx, G.M. Ferrari, J.H.W. de Wit, J.M.C. Mol, Novel time–frequency characterization of electrochemical noise data in corrosion studies using Hilbert spectra, Corros. Sci., 66 (2013) 97-110.
[21] A. Aballe, M. Bethencourt, F.J. Botana, M. Marcos, Wavelet transform-based analysis for electrochemical noise, Electrochem. Commun., 1 (1999) 266-270.
[22] R.A. Cottis, A.M. Homborg, J.M.C. Mol, The relationship between spectral and wavelet techniques for noise analysis, Electrochimica Acta, 202 (2015) 277-287.
[23] B. Zhao, J.-H. Li, R.-G. Hu, R.-G. Du, C.-J. Lin, Study on the corrosion behavior of reinforcing steel in cement mortar by electrochemical noise measurements, Electrochim. Acta, 52 (2007) 3976-3984.
[24] A.-M. Lafront, F. Safizadeha, E. Ghali, G. Houlachi, Study of the copper anode passivation by electrochemical noise analysis using spectral and wavelet transforms, Electrochim. Acta, 55 (2010) 2505-2512.
[25] A. Aballe, M. Bethencourt, F.J. Botana, M. Marcos, Using wavelets transform in the analysis of electrochemical noise data, Electrochim. Acta, 44 (1999) 4805-4816.
[26] C. Cai, Z. Zhang, F. Cao, Z. Gao, J. Zhang, C. Cao, Analysis of pitting corrosion behavior of pure Al in sodium chloride solution with the wavelet technique, J. Electroanal. Chem., 578 (2005) 143-150.
[27] T. Zhang, Y. Shao, G. Meng, F. Wang, Electrochemical noise analysis of the corrosion of AZ91D magnesium alloy in alkaline chloride solution, Electrochim. Acta, 53 (2007) 561-568.
[28] F.H. Cao, Z. Zhang, J.X Su, Y.Y Shi, J.Q Zhang, Electrochemical noise analysis of LY12-T3 in EXCO solution by discrete wavelet transform technique, Electrochim. Acta, 51 (2006) 1359-1364.
[29] J.A. Wharton, R.J.K. Wood, B.G. Mellor, Wavelet analysis of electrochemical noise measurements during corrosion of austenitic and superduplex stainless steels in chloride media, Corros. Sci., 45 (2003) 97-122.
[30] Z.-N. Yang, Z. Zhang, W.-H. Leng, K. Ling, J.-Q. Zhang, In-situ monitoring of nickel electrodeposit structure using electrochemical noise technique, Trans. Nonferrous Met. Soc. China, 16 (2006) 209-216.
[31] A.M. Homborg, R.A. Cottis, J.M.C. Mol, An integrated approach in the time, frequency and time-frequency domain for the identification of corrosion using electrochemical noise, Electrochimica Acta, 222 (2016) 627-640.
[32] N.E. Huang, Z. Shen, S.R. Long, M.C. Wu, H.H. Shih, Q. Zheng, N.C. Yen, C.C. Tung, H.H. Liu, The empirical mode decomposition and the Hilbert spectrum for nonlinear and non-stationary time series analysis, Proc. R. Soc. London, 454 (1998) 903-995.
[33] A.M. Homborg, E.P.M. van Westing, T. Tinga, G.M. Ferrari, X. Zhang, J.H.W. de Wit, J.M.C. Mol, Application of transient analysis using Hilbert spectra of electrochemical noise to the identification of corrosion inhibition, Electrochim. Acta, 116 (2014) 355-365.
[34] A.M. Homborg, C.F. Leon Morales, T. Tinga, J.H.W. de Wit, J.M.C. Mol, Detection of microbiologically influenced corrosion by electrochemical noise transients, Electrochimica Acta, 136 (2014) 223-232.
[35] A.M. Homborg, T. Tinga, X. Zhang, E.P.M. van Westing, P.J. Oonincx, G.M. Ferrari, J.H.W. de Wit, J.M.C. Mol, Transient analysis through Hilbert spectra of electrochemical noise signals for the identification of localized corrosion of stainless steel, Electrochim. Acta, 104 (2013) 84-93.
[36] S.S.Z. Mallat, Characterization of Signals from Multiscale Edges, IEEE Transactions on Pattern Analysis and Machine Intelligence, 14 (1992) 710-732.
[37] X. Ma, A.J. Peyton, Feature detection and monitoring of eddy current imaging data by means of wavelet based singularity analysis, NDT & E International, 43 (2010) 687-694.
[38] P.S.S.M.S. Venkatakrishnan, Measurement of Lipschitz Exponent (LE) using Wavelet Transform Modulus Maxima (WTMM), International Journal of Scientific & Engineering Research, 3 (2012) 1-4.
[39] J.F. Muzy, E. Bacry, A. Arneodo, Multifractal formalism for fractal signals: The structure-function approach versus the wavelet-transform modulus-maxima method, Physical Review E, 47 (1993) 875-884.

[40] S.W.L.H. Mallat, Singularity Detection and Processing with Wavelets, IEEE Transactions on Information Theory, 38 (1992) 617-643.
[41] L. Wang, M. Liang, Chatter detection based on probability distribution of wavelet modulus maxima, Robotics and Computer-Integrated Manufacturing, 25 (2009) 989-998.
[42] A. Bhatti, S. Nahavandi, Y. Frayman, 3D depth estimation for visual inspection using wavelet transform modulus maxima, Computers & Electrical Engineering, 33 (2007) 48-57.
[43] I.R. Legarreta, P.S. Addison, N. Grubb, G.R. Clegg, C.E. Robertson, K.A.A. Fox, J.N. Watson, R-wave Detection Using Continuous Wavelet Modulus Maxima, Computers in Cardiology, 30 (2003) 565-568.
[44] A. Tjirkallis, A. Kyprianou, Damage detection under varying environmental and operational conditions using Wavelet Transform Modulus Maxima decay lines similarity, Mechanical Systems and Signal Processing, 66-67 (2016) 282-297.
[45] P. Venkatakrishnan, S. Sangeetha, J.S. Gnanasekaran, M.G. Vishnukumar, A.S. Padmanaban, Analysis of Vibration in gearbox sensor data using Lipschitz Exponent (LE) function- A Wavelet approach, Third International Conference on Advances in Control and Optimization of Dynamical Systems, March 13-15 (2014) 1067-1071.
[46] C.L. Tu, W.L. Hwang, J. Ho, Analysis of Singularities From Modulus Maxima of Complex Wavelets, IEEE Transactions on Information Theory, 51 (2005) 1049-1062.
[47] A.N. Robertson, C.R. Farrar, H. Sohn, Singularity Detection for Structural Health Monitoring Using Holder Exponents, Mechanical Systems and Signal Processing, 17 (2003) 1163-1184.
[48] H. Shekarforoush, J. Zerubia, M. Berthod, Denoising by extracting fractional order singularities, IEEE International Conference on Acoustics, Speech and Signal Processing, 5 (1998) 2889-2892.
[49] S. Ritter, F. Huet, R.A. Cottis, Guideline for an assessment of electrochemical noise measurement devices, Mater. Corros., 61 (2010) 1-6.
[50] The MathWorks Inc., Wavelet Toolbox: User's Guide (R2016a), Retrieved July 1, 2016 from http://www.mathworks.com/help/pdf_doc/wavelet/wavelet_ug.pdf.
[51] The MathWorks Inc., Image Processing Toolbox: User's Guide (R2016a), Retrieved July 1, 2016 from http://www.mathworks.com/help/pdf_doc/wavelet/wavelet_ug.pdf.
[52] E. Bacry, J.F. Muzy, A. Arnéodo, Singularity spectrum of fractal signals from wavelet analysis: Exact results, Journal of statistical physics, 70 (1993) 635-674.
[53] S. Mallat, "A wavelet tour of signal processing", Academic Press, 1999.
[54] S. Jaffard, Pointwise smoothness, two-microlocalization and wavelet coefficients, Publications Matematiques, 35 (1991) 155-168.
[55] G. Berthomé, B. Malki, B. Baroux, Pitting transients analysis of stainless steels at the open circuit potential, Corros. Sci., 48 (2006) 2432-2441.
[56] G.S. Frankel, L. Stockert, F. Hunkeler, H. Boehni, Metastable pitting of stainless steel, Corrosion, 43 (1987) 429-436.
[57] Y. Li, R. Hu, J. Wang, Y. Huang, C.-J. Lin, Corrosion initiation of stainless steel in HCl solution studied using electrochemical noise and in-situ atomic force microscope, Electrochim. Acta, 54 (2009) 7134-7140.
[58] P.C. Pistorius, G.T. Burstein, Growth of corrosion pits on stainless steel in chloride solution containing dilute sulphate, Corros. Sci., 33 (1992) 1885-1897.
[59] N.J. Laycock, R.C. Newman, Localised Dissolution Kinetics, Salt Films and Pitting Potentials, Corros. Sci., 39 (1997) 1771-1790.
[60] P.C. Pistorius, G.T. Burstein, Aspects of the Effects of Electrolyte Composition on the Occurrence of Metastable Pitting on Stainless Steel, Corros. Sci., 36 (1994) 525-538.
[61] H.S. Klapper, J. Goellner, Electrochemical noise from oxygen reduction on stainless steel surfaces, Corros. Sci., 51 (2009) 144-150.

FIGURE CAPTIONS

FIGURE 1. Micrographs of an AISI304 working electrode surface exposed to an aqueous HCl solution at pH 3.0 (a), 1.9 (b) and 1.0 (c) for a duration of 1000 s

FIGURE 2. EPN signals of measurements on AISI304, exposed to an HCl solution at pH 3.0 (a), 1.9 (b) and 1.0 (c) for a duration of 1000s. Transient locations are indicated in blue

FIGURE 3. Enlargement of two sections of each 60s duration of the EN signal of Figure 2b: 120-180s (left hand side) and 800-860s (right hand side)

FIGURE 4. CWT spectra of EPN signals of measurements on AISI304, exposed to an HCl solution at pH 3.0 (a) and 1.9 (b) for a duration of 1000s

FIGURE 5a. and 5b. WTMM of the CWT spectrum from Figure 4a, indicated with black dots, in a three- (a) and two-dimensional (b) representation. FIGURE 5c. and 5d. WTMM of the CWT spectrum from Figure 4b in a three- (c) and two-dimensional (d) representation

FIGURE 6. Holder exponents of all EPN signals from the measurements of AISI304 exposed to an aqueous HCl solution at pH 1.0, 1.9 and 3.0

FIGURE 7. Probability density of Holder exponents for EN signals from experiments at pH 1.0, 1.9 and 3.0, including the Holder exponents at the x-axis

Tables

TABLE 1. Holder exponents of the EN signals from Figure 2

Signal	**Averaged Holder exponent**
pH 3.0	0,17
pH 1.9	0,70

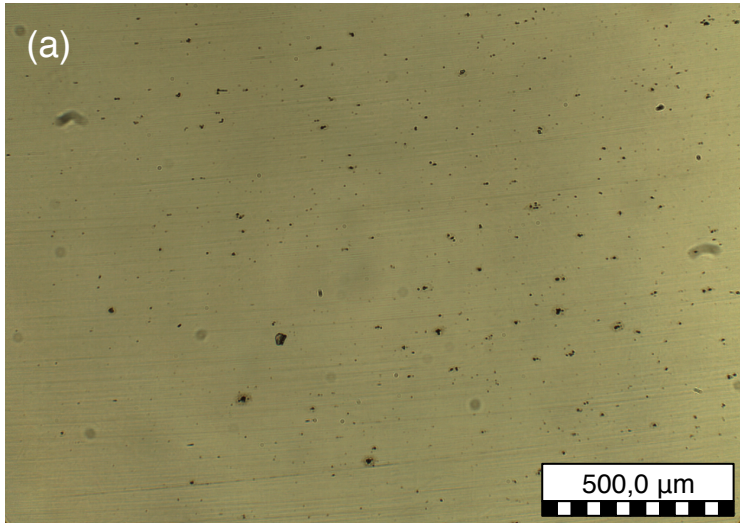

Figure 1a

Figure 1b

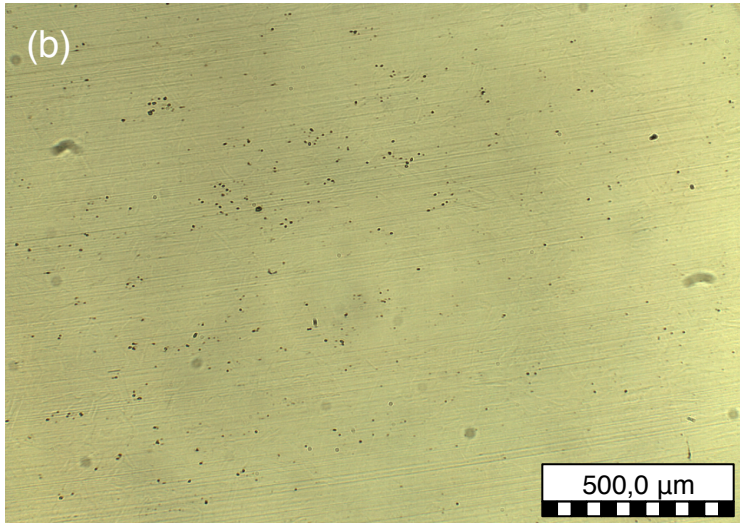

Figure 1c

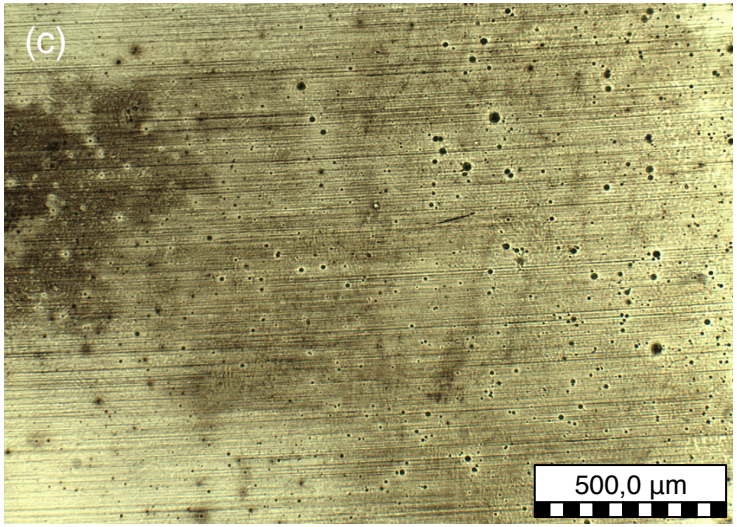

Figure 2a

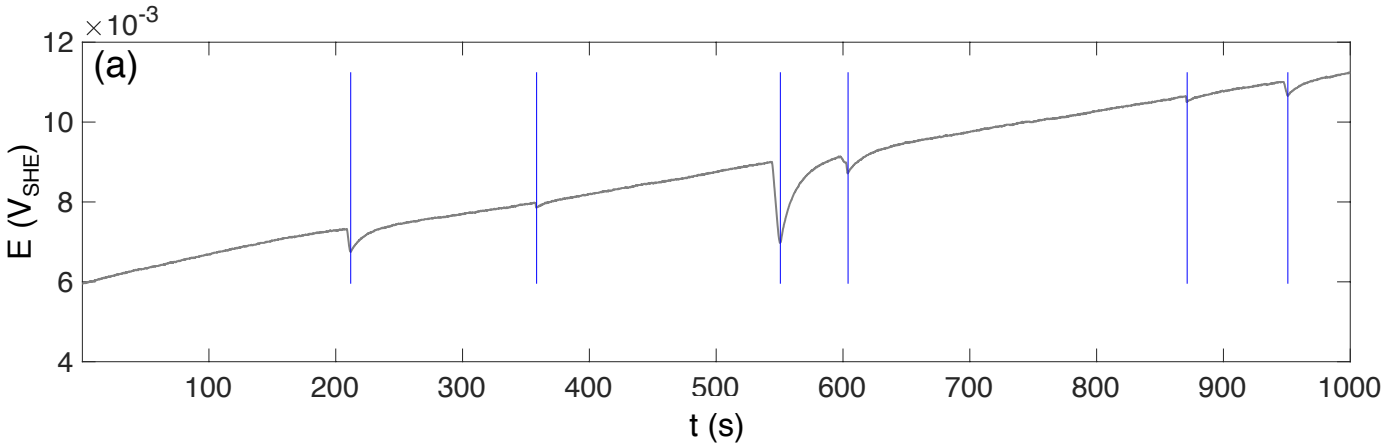

Figure 2B

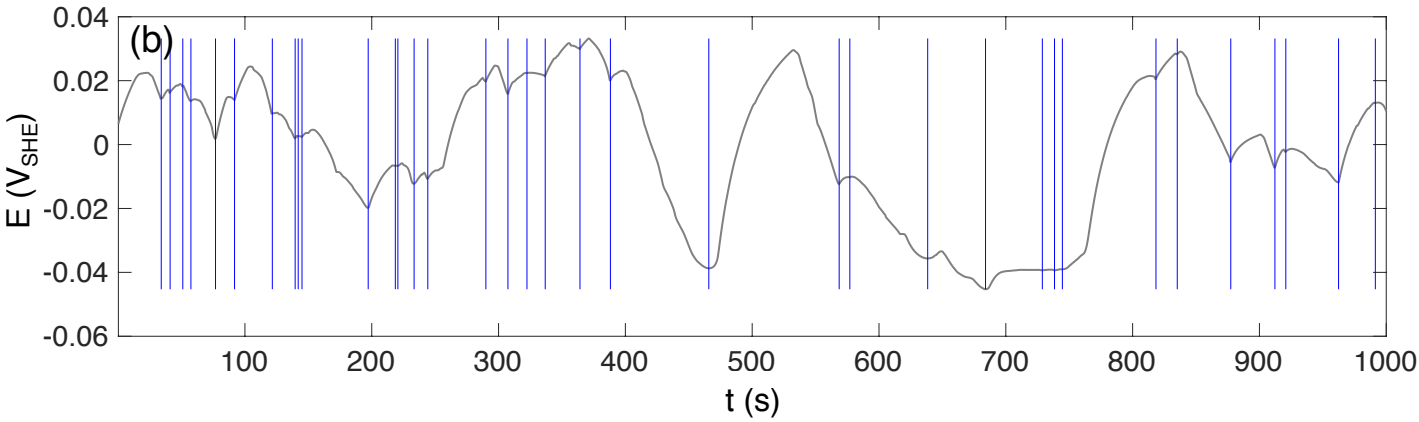
(b)
0.04
0.02
0
-0.02
-0.04
-0.06
E (V_SHE)
100
200
300
400
500
600
700
800
900
1000
t (s)

Figure 2c

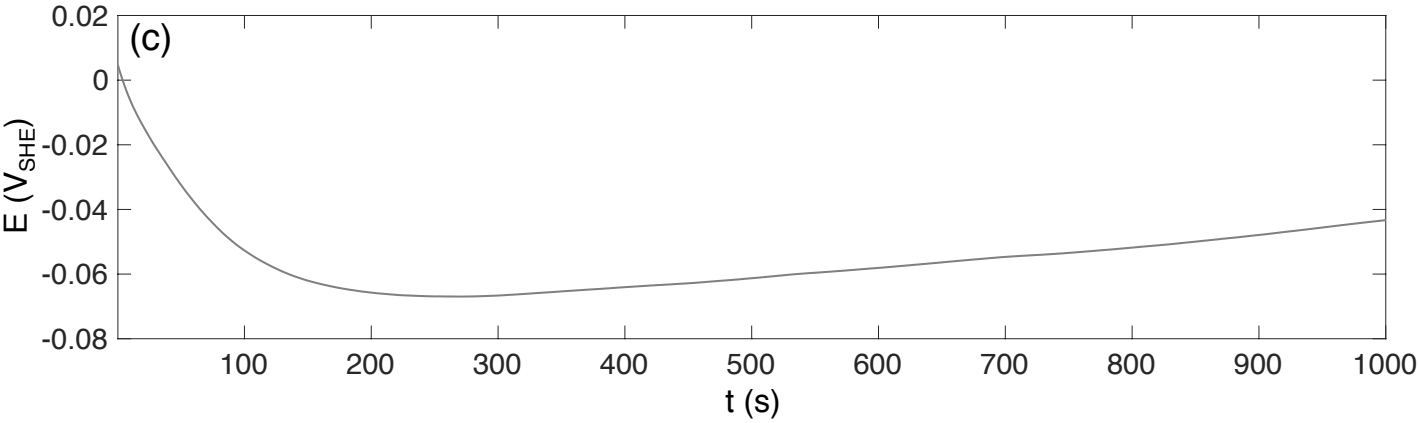
(c)
0.02
0
-0.02
-0.04
-0.06
-0.08
E (V_SHE)
100
200
300
400
500
600
700
800
900
1000
t (s)

Figure 3

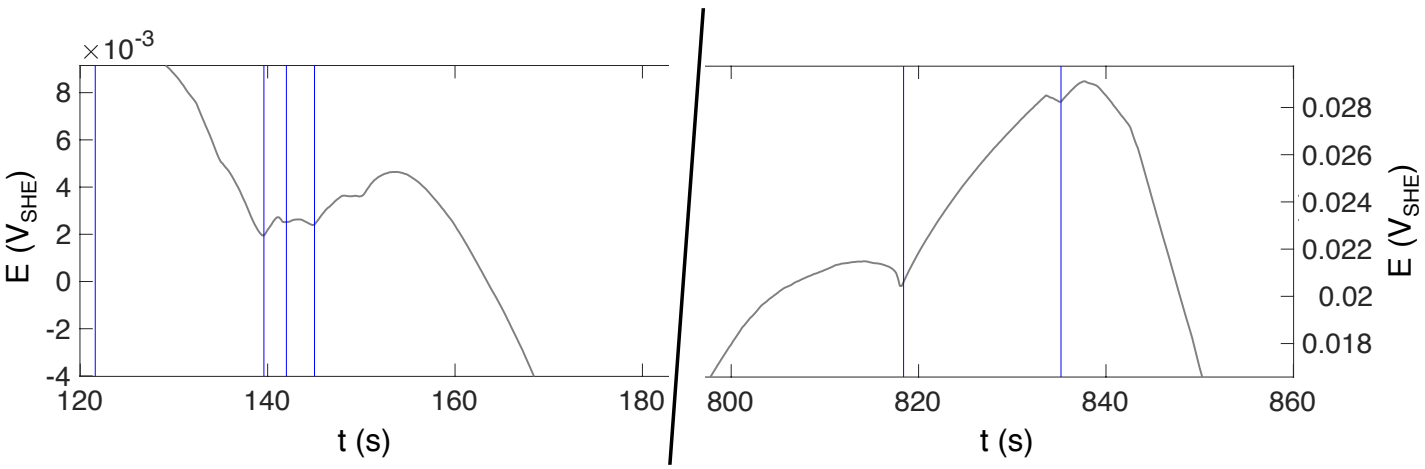
×10^-3
8
6
4
2
0
-2
-4
E (V_SHE)
120
140
160
180
t (s)
800
820
840
860
t (s)
0.028
0.026
0.024
0.022
0.02
0.018
E (V_SHE)

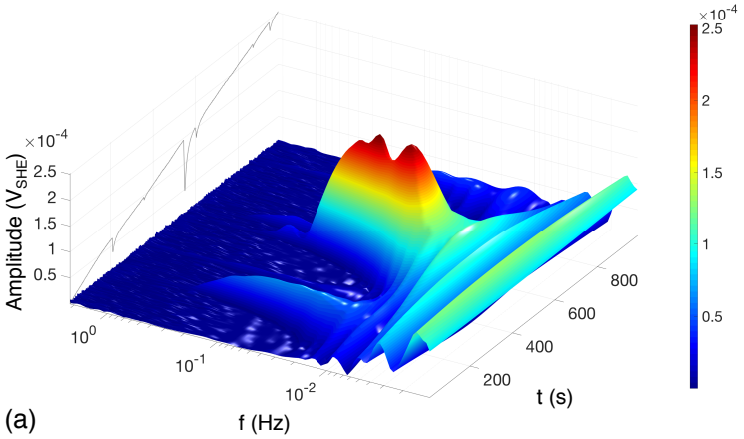
×10^-4
2.5
2
1.5
1
0.5
Amplitude (V_SHE)
10^0
10^-1
10^-2
f (Hz)
200
400
600
800
t (s)
(a)

Figure 4a

Figure 4b

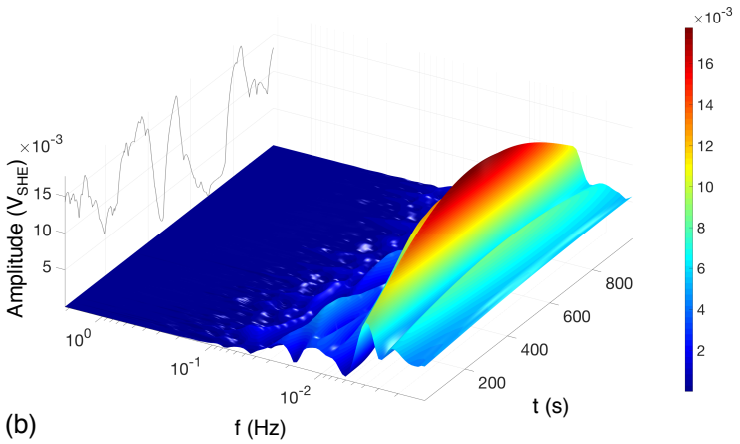
×10^-3
Amplitude (V_SHE)
15
10
5
10^0
10^-1
10^-2
f (Hz)
200
400
600
800
t (s)
×10^-3
16
14
12
10
8
6
4
2

(b)

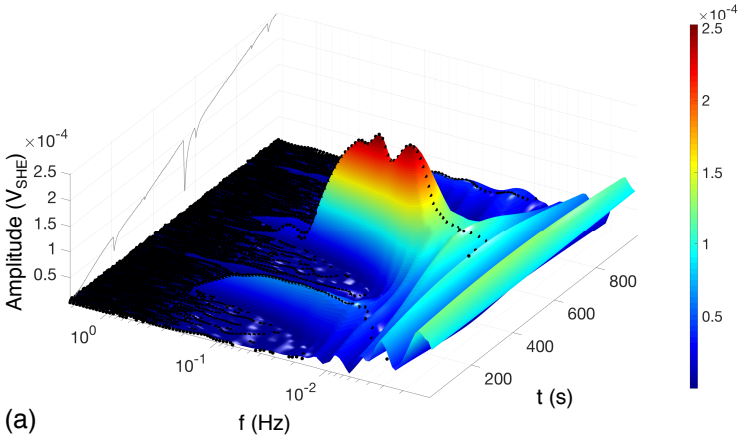
×10^-4
2.5
2
1.5
1
0.5
Amplitude (V_SHE)
10^0
10^-1
10^-2
f (Hz)
200
400
600
800
t (s)
×10^-4
2.5
2
1.5
1
0.5

(a)

Figure 5a

Figure 5b

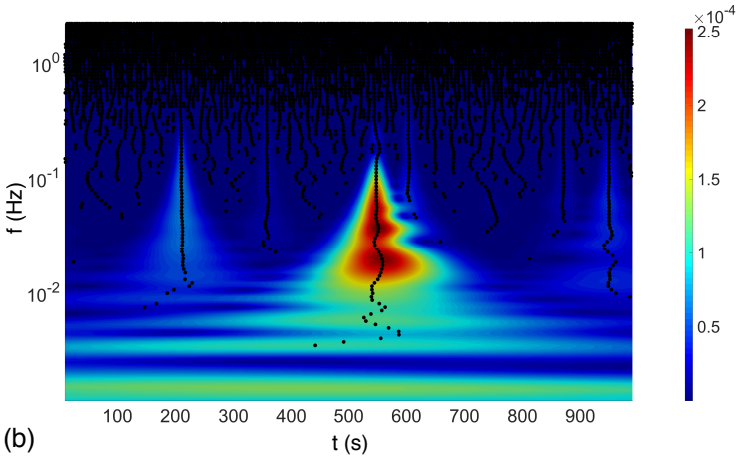
×10^-4
2.5
2
1.5
1
0.5
10^0
10^-1
10^-2
f (Hz)
100
200
300
400
500
600
700
800
900
t (s)

(b)

Figure 5c

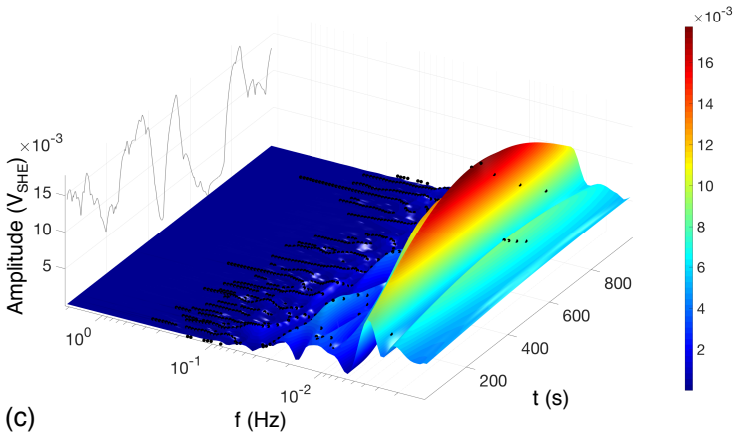
×10^-3
Amplitude (V_SHE)
15
10
5
10^0
10^-1
10^-2
f (Hz)
200
400
600
800
t (s)
×10^-3
16
14
12
10
8
6
4
2
(c)

Figure 5d

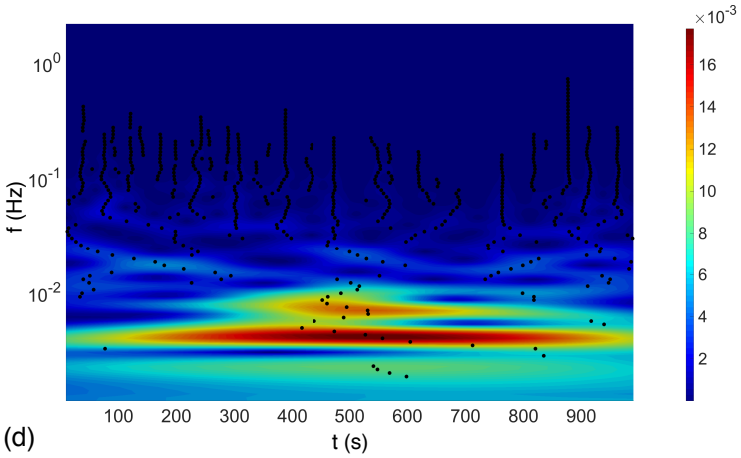
$\times 10^{-3}$
16
14
12
10
8
6
4
2
10^{0}
10^{-1}
10^{-2}
f (Hz)
100
200
300
400
500
600
700
800
900
t (s)
(d)

Figure 6

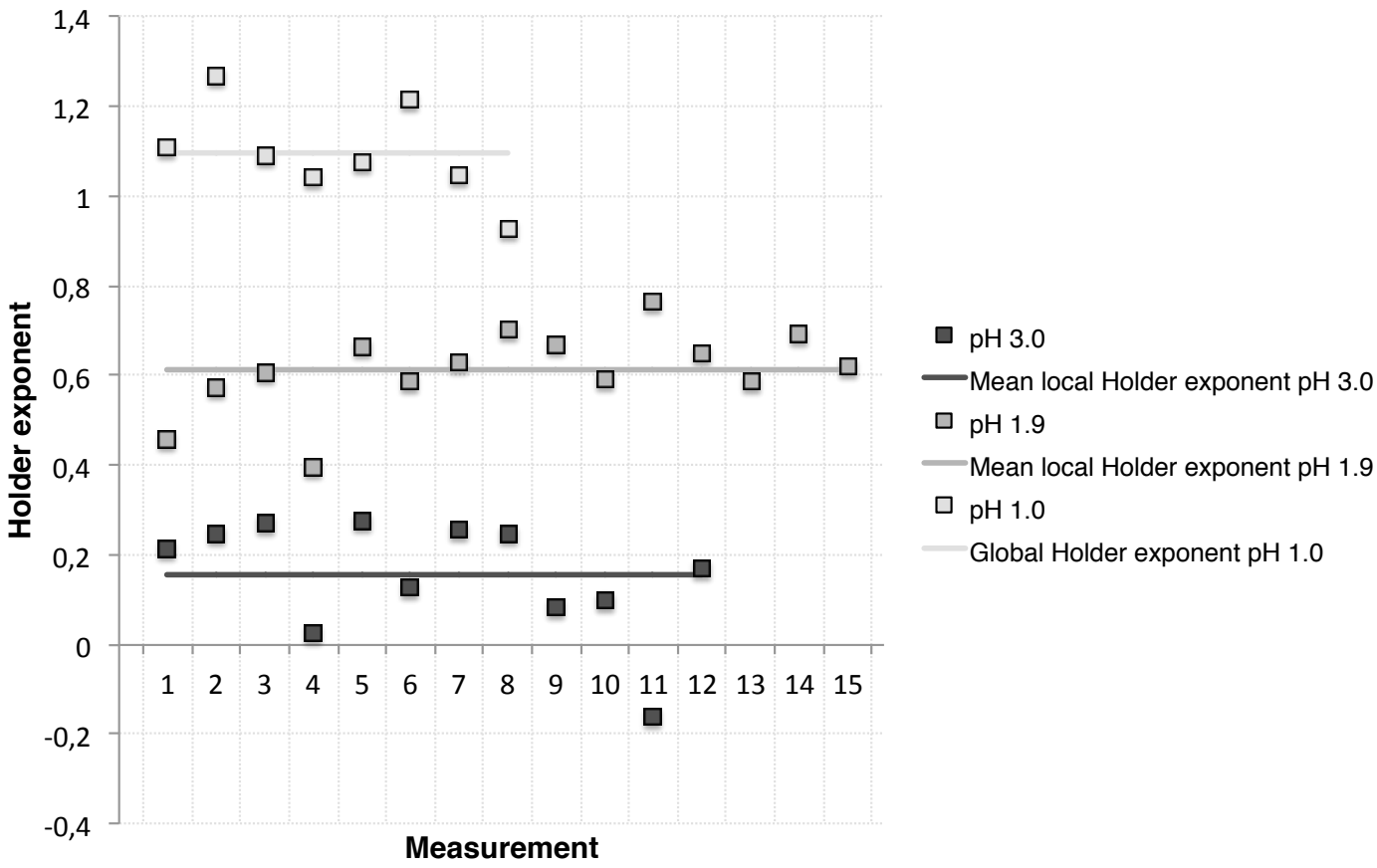
1,4
1,2
1
0,8
0,6
0,4
0,2
0
-0,2
-0,4
Holder exponent
1
2
3
4
5
6
7
8
9
10
11
12
13
14
15
Measurement
pH 3.0
Mean local Holder exponent pH 3.0
pH 1.9
Mean local Holder exponent pH 1.9
pH 1.0
Global Holder exponent pH 1.0

Figure 7

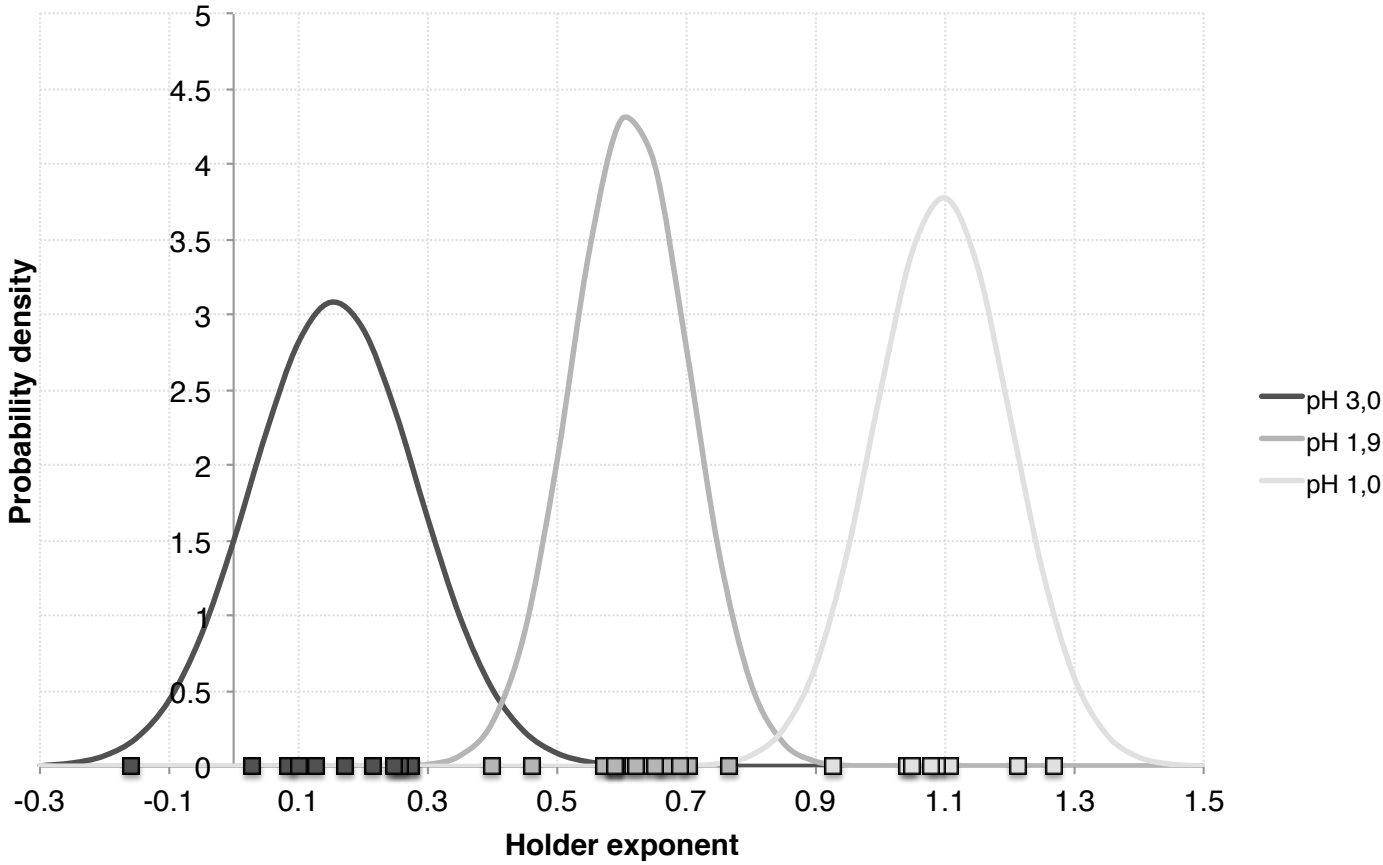
Probability density
5
4.5
4
3.5
3
2.5
2
1.5
1
0.5
0
-0.3
-0.1
0.1
0.3
0.5
0.7
0.9
1.1
1.3
1.5
Holder exponent
pH 3,0
pH 1,9
pH 1,0